

UV–Visible Absorption Spectroscopy and Photochemistry of an Alkene•O₂ Contact Charge-Transfer System in Large NaY Crystals

Sergey Vasenkov and Heinz Frei*

Laboratory of Chemical Biodynamics, MS Calvin Laboratory, Lawrence Berkeley National Laboratory, University of California, Berkeley, California 94720

Received: December 17, 1996; In Final Form: March 6, 1997[⊗]

Single layers of 40 μm NaY crystals were prepared on a CaF₂ support. These are sufficiently transparent to allow recording of reactants occluded in the zeolite pores by UV–visible transmission spectroscopy for the first time. Spectra of 2,3-dimethyl-2-butene (DMB) and oxygen gas loaded into the zeolite revealed the true absorption profile of the DMB•O₂ charge-transfer contact complex. Visible-light-induced reaction was monitored by in situ Fourier transform infrared spectroscopy. Irradiation resulted in the same selective oxidation to 2,3-dimethyl-3-hydroperoxy-1-butene observed previously in highly scattering pellets of 1 μm NaY particles.

I. Introduction

Recent photochemical studies of hydrocarbon–oxygen gas mixtures loaded into alkali or alkaline earth zeolite Y have shown that partial oxidation can be induced by visible light.¹ The primary photoproduct is the corresponding alkyl, allyl, or benzyl hydroperoxide, which is produced at (or very close to) 100% selectivity even at high conversion of the hydrocarbon. These hydroperoxides dehydrate spontaneously to the corresponding aldehyde or ketone, which are commercially important products. In cases where the hydroperoxide lacks an $\alpha\text{-H}$, the intermediate is stable and can be used in situ for stereospecific thermal epoxidation of olefins at ambient temperature.^{1f} Reflectance spectroscopy of zeolite pellets loaded with oxygen and hydrocarbon revealed a weak, continuous absorption tail in the visible region which is responsible for the photochemistry. We have shown that this absorption originates from hydrocarbon•O₂ collisional pairs. The onset of the tail scales with the ionization potential of the hydrocarbon and the strength of the zeolite electrostatic field which is the basis of our assignment to a hydrocarbon•O₂ contact charge-transfer absorption.^{1d} It is the very high electrostatic field inside the supercages of dehydrated alkali or alkaline-earth zeolite Y (NaY, 0.3 V \AA^{-1} ; BaY, 0.9 V \AA^{-1})² that causes the large red shift of alkane, alkene, or toluene•O₂ charge-transfer transitions from the UV into the visible range.¹ Absence of solvent is essential since the concentration of O₂ in solution is small (millimolar or lower), and the dielectric property of the liquid strongly reduces the Coulombic interactions. Visible-light-induced photooxidations of alkenes in zeolite pores can be accomplished in the presence of a solvent if photosensitizers are used. Sensitized electron-transfer and singlet oxygen photooxidations of olefins have recently been demonstrated in liquid suspensions of zeolites by Ramamurthy and co-workers, and high regioselectivities for hydroperoxide products were reported.³

Self-supporting zeolite Y pellets used thus far in our work consist of approximately 1 μm crystallites and therefore strongly scatter visible light. Hence, optical studies were limited to reflectance measurements.^{1d} The profile of the reflectance spectrum is dictated by the wavelength dependence of the absorption and the scattering coefficient. Therefore, it is difficult to determine the shape of the visible hydrocarbon•O₂ absorption profile from these measurements.

In order to determine the profile of the hydrocarbon•O₂ contact charge-transfer absorption in zeolites, transmission measurements have to be conducted on zeolite matrices which are transparent in the visible. For particles with grain size large compared to the probe wavelength, the scattering coefficient is inversely proportional to the grain size.⁴ Therefore, transparency in the visible is the better the larger the zeolite crystal. We have succeeded in preparing monolayers (films) of 40 μm NaY crystals that are sufficiently transparent to allow transmission measurements in the UV–visible region. In this paper, we report the results of transmission spectroscopy of the 2,3-dimethyl-2-butene + O₂ system in such a transparent NaY film. The quantum yield to visible-light-induced reaction in these films is compared with that of the same reaction in a pressed pellet of 1 μm NaY crystallites.

II. Experimental Section

Tightly packed monolayers of 40 μm NaY crystals were prepared on a CaF₂ window. The large zeolite crystals were kindly supplied to us by Dr. David Young, University of Toronto, who prepared them according to the method described by Charnell.⁵ For preparation of the NaY film, 10 mg of zeolite crystals was suspended in 50 μL cyclohexane, and the suspension was spread over a polished CaF₂ window of 1 in. diameter. Cyclohexane was chosen because it does not dissolve NaY or CaF₂ and because it could easily be removed from the zeolite pores by evacuation. In order to obtain dense, homogeneous monolayers of NaY crystals, the CaF₂ window carrying the cyclohexane suspension was covered by a second CaF₂ window. The two plates were rotated against each other for about 2 min, which led to a homogeneous distribution of crystals. Subsequent sliding away sideways of one window resulted in a compact NaY layer on one of the two plates. The layer was inspected visually by using a $\times 200$ optical microscope. Best results gave monolayers with the gaps between the crystals making up no more than 5–10% of the area. Typically, the procedure had to be repeated several times to achieve such high coverage.

UV–visible and infrared transmission spectroscopy of molecules occluded in NaY was conducted by using a miniature vacuum cell described previously.^{1b} The cell was equipped with two CaF₂ windows, one of which carried the NaY film facing the interior of the cell. The cell was mounted in a variable temperature vacuum system (Model Oxford DN 1714) with a tuning range from 77 K to 473 K. The zeolite film was

[⊗] Abstract published in *Advance ACS Abstracts*, May 15, 1997.

dehydrated by heating the cell to 200 °C for 12–15 h under evacuation to 10^{-6} Torr (turbomolecular pump Model Varian V-60). 2,3-Dimethyl-2-butene (DMB) was loaded into the zeolite from the gas phase by exposing the film to 10 Torr of hydrocarbon gas at 130 °C for 12 h. Oxygen or nitrogen gas was loaded at –20 °C. The resulting concentration corresponded to 2–3 DMB molecules per supercage and 1–2 O₂ or N₂ molecules per three supercages on average.⁶ The long exposure of the hydrocarbon gas at elevated temperature needed to reach equilibrium loading (as monitored by infrared spectroscopy) is characteristic for such large zeolite crystals.⁷

UV–visible spectra of the NaY films were recorded with a Shimadzu spectrometer Model 2100 in the standard transmission mode. In addition, transmittance spectra were taken using an integrating sphere Model ISR-260 with BaSO₄ as reference. These measurements allowed us to collect and analyze all the light transmitted through the NaY layer, including scattered light transmitted through the crystals and light diffracted at the gaps between the particles. The spectra were recorded in two different ways. First, the direct (unscattered) beam of transmitted light was blocked by a black absorber in order to record the scattered and diffracted part of the transmitted light only. Then, the direct sample beam was diffusely reflected off BaSO₄ in order to record all light (scattered, diffracted, and unscattered) transmitted through the film. Reflectance spectra of powders and pressed pellets of 1 μ m NaY crystallites were also recorded. The photochemistry was monitored in situ by FT-IR transmission spectroscopy using a Bruker Model IFS 113 instrument. For photolysis a prism-tuned CW Ar ion laser was used (Coherent Model Innova 90-6). The light beam was expanded so as to illuminate the entire zeolite film.

2,3-Dimethyl-2-butene (Aldrich, 99%) was vacuum-distilled before use. Oxygen and nitrogen gas (Air Products, 99.997%) and cyclohexane (Aldrich, 99%) were used as received. Zeolite NaY (LZ-Y52, Aldrich Lot. No. 12929CN) consisting of small (about 1 μ m) crystallites was employed for recording of spectra of pressed pellets for the purpose of comparison.

III. Results and Discussion

1. Transmittance Spectra of NaY Films. A UV–visible transmittance spectrum of a dehydrated film of 40 μ m NaY crystals mounted inside the vacuum cell is shown in Figure 1a. The spectrum was measured with standard spectrometer optics (no integrating sphere) and referenced against the empty optical cell. Hence, the y axis represents the combined light transmitted through the crystals and bypassing them through the small gaps in between (only undiffracted part). However, it does not comprise all the light that goes through the crystals or gaps because a substantial fraction of that light is scattered and therefore does not reach the detector or is diffracted at the gaps (see below). Nevertheless, the spectrum reveals several noteworthy points: (i) no distinct absorption is observed at $\lambda > 300$ nm, which confirms the well-known fact that zeolite NaY has no optical absorption in the visible;⁸ (ii) the transmittance increases steadily toward shorter wavelengths until it levels off and decreases around 300 nm. The wavelength dependence at $\lambda > 300$ nm could originate from a change of the scattering coefficient and/or a change of the regular reflection of the crystals. Alternatively, it could be caused by the wavelength dependence of the diffraction at the gaps between the crystals. A distinction between the two possibilities can be made on the basis of transmission measurements using the integrating sphere. (The wavelength dependence at $\lambda < 300$ nm will be discussed in section III.3.)

The upper curve of Figure 1b (trace 1) shows the transmittance spectrum of the same layer of 40 μ m NaY crystals

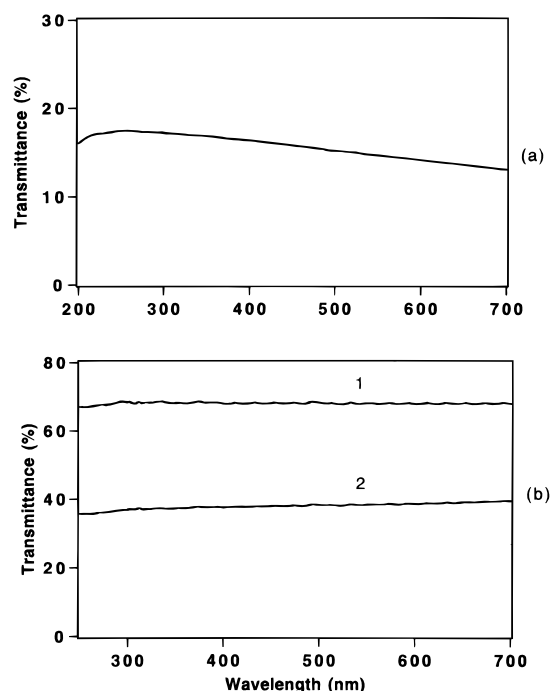


Figure 1. (a) UV–visible transmittance spectrum of a dehydrated 40 μ m NaY film at 253 K. Only light transmitted in the direction of the incident beam was recorded. Reference is the empty optical vacuum cell. (b) UV–visible transmittance spectrum of a hydrated 40 μ m NaY film at 295 K recorded with an integrating sphere (reference BaSO₄). Curve 1, scattered and unscattered transmitted light. Curve 2, scattered transmitted light only.

displayed in Figure 1a, except that this time all the light emerging from the rear surface of the film was collected. To record this spectrum, no optical cell could be used, and the measurement had to be conducted with the film in its hydrated state. The experimental setup consists of an integrating sphere configured such that both scattered and unscattered light from the sample are detected (see section II). Barium sulfate was used as white standard. When the unscattered sample beam was blocked by an absorber, the second spectrum of Figure 1b was obtained (trace 2). This corresponds to the light transmitted through the crystals emerging from the film at some angle because of refraction, plus the light diffracted at the gaps. According to trace 1, the total light transmitted through the film (scattered and unscattered) is constant across the 300–700 nm range. This implies that the reflection of the NaY crystals is wavelength independent and that, therefore, the scattering coefficient and regular reflection, and thus the refractive index of the crystal, are constant over this wavelength range.⁴ Hence, we attribute the slight decrease of the scattered/diffracted fraction of the transmitted light with decreasing wavelength (trace 2 of Figure 1b) to less diffraction of the light at the gaps between the crystals.⁹ This is consistent with our estimate of a 2–4 μ m average size of the gap, which we derived from an estimated 90–95% surface coverage of the 40 μ m crystals in a typical film. We conclude, therefore, that the slight increase of the transmittance of the NaY film in Figure 1a with decreasing wavelength is due to a decrease in diffraction at the gaps.

With the UV–visible base line of the zeolite layer established, it is straightforward to interpret the spectrum upon loading of the hydrocarbon. Figure 2 shows the absorbance difference spectrum at –20 °C before and after loading of DMB into the NaY film. Standard transmission optics was used. Gas phase molecules were removed by evacuation. (At –20 °C, desorption of DMB from these large NaY crystals by evacuation is very slow.) Hence, the observed band is due to zeolite-adsorbed

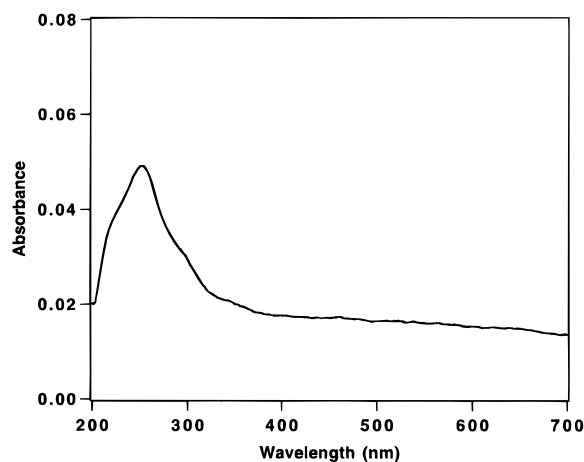


Figure 2. UV-visible absorbance difference spectrum at 253 K recorded upon loading of 2,3-dimethyl-2-butene into a 40 μm NaY film. Only light transmitted in the direction of the incident beam was recorded.

hydrocarbon only as verified by infrared monitoring (see section III.2). The UV band with a maximum at 250 nm is attributed to excitation of the S₁ state of DMB. The onset around 370 nm coincides with the onset of the same band in the liquid olefin.¹⁰ In addition to the DMB absorption, a base line shift of about 0.02 absorbance units across the entire UV and visible region is noted. This shift is similar for other small olefins occluded in these NaY films (such as 2-butene) and is caused by a change of the refractive index of the zeolite upon occlusion of the hydrocarbon.¹¹ The base line shift obscures the exact onset of the DMB absorption tail.

Loading of the cell with several atmospheres of O₂ led to a base line shift in the UV-visible due to Rayleigh scattering. In addition, a slight shift might have originated from the influence of occluded O₂ on the zeolite refractive index. Therefore, taking the mere difference of spectra before and after exposure of the DMB-loaded NaY film to O₂ gas would not reveal the true shape of the DMB•O₂ charge-transfer absorption. We conducted experiments with N₂ as an inert gas to compensate for these effects. First, the NaY film was exposed to N₂ (4.9 atm) at 253 K and a transmittance spectrum recorded. Then, N₂ was pumped off and replaced by 4.9 atm of oxygen. Subtraction of the N₂/NaY transmittance spectrum from the O₂/NaY spectrum gives the difference of Rayleigh scattering, optical absorption (at $\lambda < 260$ nm), and possibly slight refractive index effect of O₂- and N₂-loaded cell and film (Figure 3, trace 1). We chose subtraction instead of division of the transmittance spectra in order to eliminate any effect of the light transmitted through the gaps between the crystals. In particular, this procedure removed completely any distortion of the spectrum by the wavelength dependence of diffracted/undiffracted light passing through the gaps (Figure 1a). Spectral trace 1 is the average of 14 O₂ and N₂ loading experiments. The absorption at $\lambda < 260$ nm is due to gas phase O₂.¹² Taking an analogous sequence of spectra upon exposure of a DMB-loaded NaY film to N₂ and O₂ (4.9 atm) at 253 K resulted in spectrum 2 of Figure 3 (average of 18 such N₂ and O₂ loading experiments). The insert of Figure 3 shows the extreme traces of the range of spectra taken into account in determining the average; there is no negative contribution to the average even from the trace with the lowest recorded signal. The difference between curve 2 and curve 1 of Figure 3 represents the true profile of the DMB•O₂ absorption in zeolite NaY. It shows an onset between 600 and 700 nm and a very flat maximum between 400 and 500 nm. The intensity of the absorption, however, understates the fraction of light absorbed by the DMB•O₂ pairs by a

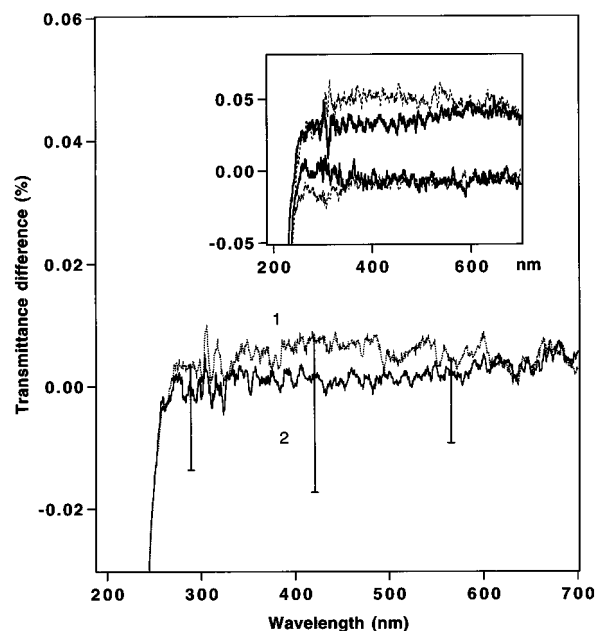


Figure 3. UV-visible transmittance spectra O₂-N₂/NaY (curve 1) and DMB/O₂-N₂/NaY (curve 2) for films of large crystals at 253 K (see text for details). The difference of the two spectra shows the DMB•O₂ absorption normalized to the incident light. Only light transmitted in the direction of the incident beam was recorded. The bars indicate the estimated DMB•O₂ absorption for scattered and unscattered transmitted light, which is used for quantum efficiency determination. The insert shows the extreme spectra (smallest and largest) from the range of spectra accumulated and used for the calculation of traces 1 and 2.

substantial factor. The reason is that Figure 3 shows differences of transmittances; hence, the absorption is proportional to the fraction of the transmitted light captured by the detector. Because of the vacuum cell, only unscattered light could be recorded in the experiment reported in Figure 3. Comparison of parts a and b of Figure 1, curve 2, indicates that the scattered fraction of the transmitted light is about 3 times larger than the unscattered part. This means that only 25% of the transmitted light was recorded in the experiment shown in Figure 3. Therefore, the actual absorption of DMB•O₂ reactants is 4 times stronger and is indicated by the bars in Figure 3. For the purpose of control, we compared the spectra of DMB-loaded NaY before and after the O₂ and N₂ loading cycles and spectroscopy but did not notice any spectral changes. Therefore, the difference between curve 2 and curve 1 cannot be due to any accumulated thermal products or species generated by irradiation with the UV-visible spectrometer source.

2. Photochemical Reaction. Loading of DMB into a NaY film produced the infrared spectrum shown in Figure 4a. Absorptions at 1368 (shoulder), 1380, 1398, 1449, 2740, 2870, 2920, and 2990 cm⁻¹ essentially coincide with the bands of DMB in pressed pellets of 1 μm NaY crystallites reported earlier.^{1a,b} The temperature of the film was 223 K. Gas phase olefin was removed by evacuation. We found that no desorption of DMB took place over a period of at least 5 h when keeping the NaY film at 223 K or lower.

The DMB/NaY infrared spectrum of Figure 4a is the result after base line correction. The raw spectrum exhibits a steep slope in the spectral region shown. Apparently, the closeness of probe wavelength (6–8 μm) and NaY crystal size (40 μm) has a substantial effect on the wavelength dependence of the scattering coefficient upon DMB loading of the crystals. By contrast, subsequent exposure to O₂ gas did not affect the infrared spectrum.

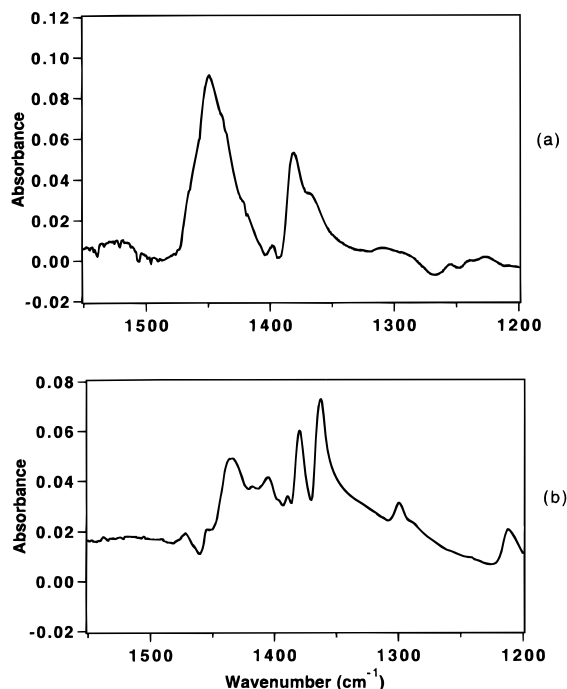


Figure 4. (a) FT-IR difference spectrum upon loading of DMB into 40 μm NaY film (after base line correction). (b) Infrared difference spectrum following photolysis of the DMB and O_2 -loaded film at 223 K with 515 nm light (2 h at 400 mW cm^{-2}).

Irradiation of the DMB/ O_2 /NaY film with green light (515 nm, 400 mW cm^{-2}) for 2 h resulted in the infrared difference spectrum shown in Figure 4b. Depletion of DMB is observed under concurrent absorbance growth at 1299, 1362, 1378, 1388, 1404, 1434, 1625, and 1633 cm^{-1} (shoulder). Identification of the product as DMB hydroperoxide (2,3-dimethyl-3-hydroperoxy-1-butene) is unambiguous because the spectrum is identical with that of an authentic sample of the hydroperoxide occluded in a pressed NaY pellet.^{1b} No other product appeared. (The peak at 1210 cm^{-1} , obscured in pressed pellets by zeolite absorption, agrees with the spectrum of DMB hydroperoxide reported in the literature.¹³) The growth upon 2 h of green light photolysis shown in Figure 4b amounts to conversion of more than half of the loaded DMB to hydroperoxide, yet no byproduct is observed. We conclude that in 40 μm NaY crystals the same visible-light-induced reaction occurs between DMB and O_2 as in pressed pellets of 1 μm NaY particles.^{1a,b}

3. UV-Visible Transmittance of NaY Pellets. In order to compare the DMB· O_2 UV-visible absorption in the 40 μm NaY particles with that of DMB· O_2 occluded in a pressed pellet of 1 μm NaY crystallites reported earlier,^{1d} measurement of the transmittance spectrum of the pellet was required. Pellets were between 5 and 10 mg with a diameter of 12 mm and a thickness of 50–100 μm . As reported previously, less than 0.1% of the UV or visible light is transmitted through the pellet in the direction of the incident light.^{1d} Measurement of the transmittance with the integrating sphere allowed us to determine the total light transmitted through the pellet. This experiment was conducted with a hydrated film in air because use of the miniature optical vacuum cell prevents collection of the scattered light of the pellet. The result, shown in curve 1 of Figure 5a, indicates a decrease from 31% transmittance at 700 nm to 12% at 300 nm, to 1% at 250 nm. Hence, in the visible spectral range the average transmittance is around 25%. The close to linear decrease of the transmittance toward shorter wavelengths between 700 and 300 nm is mirrored by a corresponding increase of the reflectance over the same spectral range, shown in curve 2 of Figure 5a. This is in agreement with Mie theory

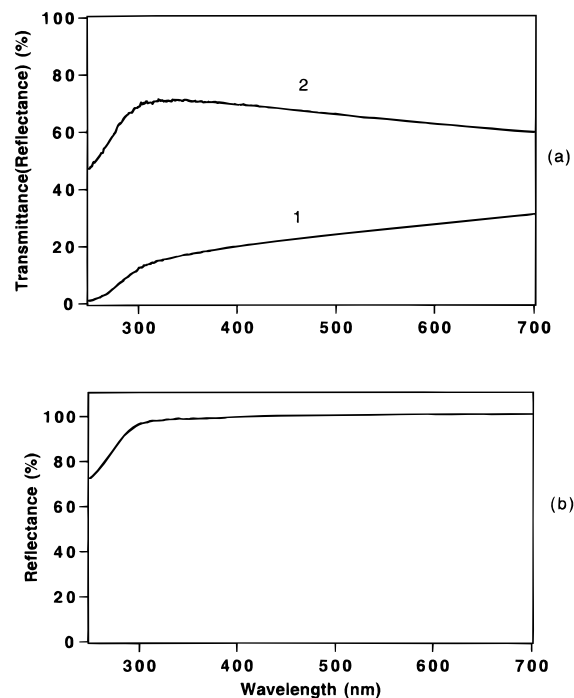


Figure 5. (a) Curve 1: UV-visible transmittance spectrum of a pressed pellet of hydrated 1 μm NaY particles at 295 K recorded with an integrating sphere (reference, BaSO_4). Curve 2: reflectance spectrum of the same pellet. (b) Diffuse reflectance spectrum of a powder of 1 μm NaY particles. BaSO_4 was used as reference.

according to which the scattering coefficient and, hence, the transmittance and reflectance depend on the wavelength when it is close to the particle size.

To establish the origin of the sharp decrease of the transmittance and reflectance of the pressed NaY pellet at $\lambda < 320$ nm (Figure 5a), a diffuse reflectance spectrum of NaY powder was recorded (Figure 5b). The powder layer was prepared sufficiently deep (about 4 mm) to prevent any light from escaping the rear surface of the layer. The diffuse reflectance shows practically no wavelength dependence in the visible and near-UV to about 300 nm but decreases precipitously at $\lambda < 300$ nm. The spectrum was not sensitive to the angle between the direction of the incident light beam and the surface of the NaY powder (82°, 90°, and 98° angles were used), indicating that regular reflection does not change across the recorded region. This leaves optical absorption by NaY as the only explanation for the reflectance decrease at $\lambda < 320$ nm. We conclude that the signal decrease in Figures 5a,b and 1 (spectrum of the NaY (40 μm) film) is due to absorption by the zeolite. This is in agreement with the NaY absorption onset reported in the literature.¹⁴

It is interesting to compare the DMB· O_2 charge-transfer spectra of 40 μm NaY films with the reflectance spectra of the DMB· O_2 system in pressed NaY pellets. The shape of the charge-transfer absorption shown in Figure 3 represents the wavelength dependence of the absorption coefficient because the scattering coefficient and the regular reflection of the large NaY crystals do not depend on wavelength (section III.1). In the case of the pressed NaY pellet, by contrast, the scattering coefficient increases toward shorter wavelengths (Figure 5a). This results in more extensive multiple scatterings, which tends to increase the average photon path length. Thus, the apparent absorption coefficient of the DMB· O_2 charge-transfer transition is expected to increase toward shorter wavelengths. We attribute the much steeper wavelength dependence of the DMB· O_2 absorption in the reflectance spectrum of the NaY pellet (ref

1d, Figure 2a) compared to the 40 μm NaY film (Figure 3) mainly to this effect. An additional distortion of the profile of the DMB•O₂ absorption in the case of the pressed pellet may originate from the fact that transmitted light was not measured and from the use of a vacuum cell for holding the pellet, which prevented collection of all reflected light by the integrating sphere.^{1d} Only reflected light inside a cone with a narrow solid angle reached the sphere. At wavelengths with low scattering coefficients the average photon path may depend on the reflection angle, which could lead to a further distortion of the DMB•O₂ absorption profile.

4. Reaction Quantum Yield in NaY Film. The product growth per absorbed photon was calculated from the infrared absorbance growth of the alkene hydroperoxide, the DMB•O₂ absorption (Figure 3), and the photon flux. Measurements were done under loading conditions and temperature of the experiment described in Figure 3. Irradiation at 514 nm with 6.7×10^{-3} mol photons (65 min at 400 mW cm⁻²) resulted in hydroperoxide growth at 1368 cm⁻¹ of 0.0030 absorbance units. According to a previous recording of an authentic sample of 2,3-dimethyl-3-hydroperoxy-1-butene loaded into NaY, this corresponds to 5.1×10^{-8} mol of hydroperoxide.^{1d} The absorption of DMB•O₂ at 514 nm is 0.02% according to Figure 3, which implies that 1.3×10^{-6} mol of photolysis photons was absorbed by the reactants. Therefore, the quantum yield of the DMB + O₂ reaction at 514 nm is 0.04. We estimate an uncertainty of a factor of 3 for the quantum yield because of the weak DMB•O₂ absorption at 514 nm and the uncertainty in estimating the fraction of the scattered light and its path length.

Determination of the DMB + O₂ reaction quantum yield for the case of the pressed NaY pellet gave a value of 0.18.^{1d} While of the same order of magnitude, the difference between the quantum yields for pellet and large crystals lies outside the random uncertainties. A likely source of systematic error lies in the reflectance measurements on pressed pellets. Only light reflected in a narrow cone around the incident spectrometer beam reaches the integrating sphere. All other reflected light and all transmitted light are not recorded. The average path length of the recorded light may be shorter than that of light transmitted through the pellet or penetrating into the pellet but reflected at an angle outside the cone. The result would be an underestimation of the amount of photolysis light absorbed and hence an overestimation of the quantum efficiency.

IV. Conclusions

UV-visible transmission spectroscopy of 2,3-dimethyl-2-butene•O₂ contact complexes inside the cages of large NaY

crystals revealed the true profile of the hydrocarbon-oxygen charge-transfer absorption in the zeolite. The absorption extends into the red spectral range, confirming the result of previous reflectance measurements on pressed pellets of small NaY crystallites.^{1d} The agreement of the spectroscopic results and the observed photoproduct in the two optically very different zeolite forms (large crystal film and pressed pellet of small particles) adds strong support to our assignment of the visible-light-induced oxidation in terms of hydrocarbon•O₂ charge-transfer photochemistry.

Acknowledgment. This work was supported by the Director, Office of Energy Research, Office of Basic Energy Sciences, Chemical Sciences Division of the U.S. Department of Energy, under Contract DE-AC03-76-SF00098. The authors thank Dr. David Young, University of Toronto, for a generous gift of 40 μm NaY crystals.

References and Notes

- (1) (a) Blatter, F.; Frei, H. *J. Am. Chem. Soc.* **1993**, *115*, 7501. (b) Blatter, F.; Frei, H. *J. Am. Chem. Soc.* **1994**, *116*, 1812. (c) Sun, H.; Blatter, F.; Frei, H. *J. Am. Chem. Soc.* **1994**, *116*, 7951. (d) Blatter, F.; Moreau, F.; Frei, H. *J. Phys. Chem.* **1994**, *98*, 13403. (e) Blatter, F.; Sun, H.; Frei, H. *Catal. Lett.* **1995**, *35*, 1. (f) Blatter, F.; Sun, H.; Frei, H. *Chem. Eur. J.* **1996**, *2*, 385; *Angew. Chem., Int. Ed. Engl.* **1996**, *35*. (g) Sun, H.; Blatter, F.; Frei, H. *J. Am. Chem. Soc.* **1996**, *118*, 6873. (h) Frei, H.; Blatter, F.; Sun, H. *CHEMTECH* **1996**, *26*, 24. (i) Sun, H.; Blatter, F.; Frei, H. In *Heterogeneous Hydrocarbon Oxidation*; Oyama, S. T.; Warren, B. K., Eds.; ACS Symposium Series No. 638; American Chemical Society: Washington, DC, 1996; p 409.
- (2) Blatter, F.; Frei, H. To be submitted.
- (3) (a) Li, X.; Ramamurthy, V. *Tetrahedron Lett.* **1996**, *37*, 5235. (b) Li, X.; Ramamurthy, V. *J. Am. Chem. Soc.* **1996**, *118*, 10666.
- (4) Kortum, G. *Reflectance Spectroscopy*; Springer: Berlin, 1969; pp 81, 191.
- (5) Charnell, J. F. *J. Cryst. Growth* **1971**, *8*, 291.
- (6) Breck, D. W. *Zeolite Molecular Sieves: Structure, Chemistry, and Use*; Wiley: New York, 1974; Chapter 8.
- (7) Kärger, J.; Ruthven, D. M. *Diffusion in Zeolites*; Wiley: New York, 1992; Chapter 13.
- (8) Engel, S.; Kynast, U.; Unger, K. K.; Schüth, F. In *Zeolites and Related Microporous Materials, Studies in Surface Science and Catalysis*; Weitkamp, J., Karge, H. G., Pfeifer, H., Hölderich, W., Eds.; Elsevier: Amsterdam, The Netherlands, 1994; Vol. 84, p 477.
- (9) Hapke, B. *Theory of Reflectance and Emittance Spectroscopy*; Cambridge University Press: New York, 1993; p 78.
- (10) Itoh, M.; Mulliken, R. S. *J. Phys. Chem.* **1969**, *73*, 4332.
- (11) Reference 6, p 320.
- (12) (a) Herzberg, G. *Spectra of Diatomic Molecules*; Van Nostrand: New York, 1950; p 560. (b) Buschmann, H. W. *Ber. Bunsen-Ges. Phys. Chem.* **1974**, *78*, 1344.
- (13) Foote, C. S.; Wexler, S.; Ando, W.; Higgins, R. *J. Am. Chem. Soc.* **1968**, *90*, 975.
- (14) Primet, M.; Garbowski, E.; Mathieu, M. V.; Imelik, B. *J. Chem. Soc., Faraday Trans. 1* **1980**, *76*, 1942.